Multi–Objective Optimisation of Metamaterial Antenna

James R. Capers*, Stephen J. Boyes†, Alastair P. Hibbins*, Simon A. R. Horsley*
*Centre for Metamaterial Research and Innovation, University of Exeter, Stocker Road, Exeter, United Kingdom, EX4 4QL
†DSTL, Porton Down, Salisbury, Wiltshire, United Kingdom, SP4 0JQ
jrc232@exeter.ac.uk

***Abstract*—Passive manipulation of radiation is key to many modern technologies for sensing and communication. While many techniques exist to design electromagnetic systems that perform a single desired function, the design of systems which are multi–functional remains challenging. We have developed a versatile semi–analytic framework for designing multi–functional metamaterials to shape antenna radiation. To demonstrate the versatility of this method we design two devices: one which re–shapes the radiation pattern of an emitter while also enhancing the efficiency, and one which beams radiation into different directions depending upon the polarisation of a driven element.**

***Index Terms*—antennas, electromagnetics, propagation, measurements.**

I. Introduction

Antenna systems are key to many aspects of modern life, from mobile communications to self–driving cars. The proliferation and advancement of mobile devices over the last two decades has placed increasing demand on antenna systems. For example, the miniaturisation of antenna for i.e. mobile phones, is well known to degrade performance. At the same time the increasing amount of traffic on communications networks has led to the over–crowing of telecoms frequencies. To address these challenges, improved techniques for designing efficient task–specific antenna are required.

One way to manipulate antenna radiation is using metamaterials, man–made materials structured at sub–wavelength scales. In recent years much attention has been paid to the design of metamaterials [1], particularly metamaterials that respond differently to different input fields, enabling passive mode–sorting [2], beam–steering [3] and multiplexing output beams [4]. However, the process of designing multi–functional metamaterials remains challenging. Usual approaches make use of gradient based techniques however figure of merit gradients can be numerically expensive to evaluate; even if one makes use of the adjoint method [5] several full–wave simulations are required.

In this work, we develop a methodology for designing antenna systems for a wide range of applications. Our work can be understood as a generalisation of the concepts behind the Yagi–Uda antenna. Composed of a single driven element and collection of metal rods arranged in a line in front of the driven element, the Yagi–Uda antenna produces a highly directive beam. To try to design antenna for more general functionality, we have developed a framework for placing scattering elements around an emitter to engineer the fields to achieve almost any desired effect.

II. Multi–Functional Inverse Design using the Discrete Dipole Approximation

Treating our metamaterial system as a collection of sub–wavelength dipolar scatterers, we can employ the discrete dipole approximation to model the system. Working under these approximations, we can extend recent work [6], [7] that proposed a framework for designing single–function wave–shaping devices to the design of multi–functional systems. We begin by writing Maxwell's equations for a fixed frequency $\omega = ck_0$, where k_0 is the wave–number, as

$$\mathcal{M}\begin{pmatrix}\boldsymbol{E}\\ \boldsymbol{H}\end{pmatrix} = \begin{pmatrix}\boldsymbol{E}_{\mathrm{inc}}\\ \boldsymbol{H}_{\mathrm{inc}}\end{pmatrix} + \begin{pmatrix}\omega^2\mu_0 & i\omega\mu_0\nabla\times\\ -i\omega\nabla\times & k_0^2\end{pmatrix}\begin{pmatrix}\boldsymbol{P}\\ \boldsymbol{M}\end{pmatrix} \quad (1)$$

where the vector wave operator is

$$\mathcal{M} = \begin{pmatrix}\nabla\times\nabla\times & \mathbf{0}\\ \mathbf{0} & \nabla\times\nabla\times\end{pmatrix} - k_0^2\mathbf{1}. \quad (2)$$

The metamaterial is characterised by a spatially varying polarisation density $\boldsymbol{P}$ and magnetisation density $\boldsymbol{M}$. The field from the emitter we are trying to engineer the radiaiton from is $(\boldsymbol{E}_{\mathrm{inc}}, \boldsymbol{H}_{\mathrm{inc}})^T$. Treating the metamaterial as a collection of identical point dipoles with electric polarisability $\boldsymbol{\alpha}_E$ and magnetic polarisability $\boldsymbol{\alpha}_H$, the source terms in Maxwell's equations (1) can be written as

$$\boldsymbol{P} = \sum_n \boldsymbol{\alpha}_E \boldsymbol{E}(\boldsymbol{r}_n)\delta(\boldsymbol{r}-\boldsymbol{r}_n), \quad (3)$$

$$\boldsymbol{M} = \sum_n \boldsymbol{\alpha}_H \boldsymbol{H}(\boldsymbol{r}_n)\delta(\boldsymbol{r}-\boldsymbol{r}_n). \quad (4)$$

Under these approximations, Maxwell's equations can be solved analytically using the dyadic Green's function, defined as satisfying

$$\nabla\times\nabla\times\boldsymbol{G}(\boldsymbol{r},\boldsymbol{r'}) - k^2\boldsymbol{G}(\boldsymbol{r},\boldsymbol{r'}) = \mathbf{1}\delta(\boldsymbol{r}-\boldsymbol{r'}). \quad (5)$$

The solution for the fields is

$$\phi(\boldsymbol{r}) = \phi_{\mathrm{inc}}(\boldsymbol{r}) + \sum_{n=0}^{N} G(\boldsymbol{r},\boldsymbol{r}_n)\phi(\boldsymbol{r}_n). \quad (6)$$

where we have adopted the compact notation

$$\phi(\boldsymbol{r}) = \begin{pmatrix} \boldsymbol{E}(\boldsymbol{r}) \\ \eta_0 \boldsymbol{H}(\boldsymbol{r}) \end{pmatrix} \tag{7}$$

$$G(\boldsymbol{r}, \boldsymbol{r'}) = \begin{pmatrix} \xi^2 \boldsymbol{G}(\boldsymbol{r}, \boldsymbol{r'}) \boldsymbol{\alpha}_E & i\xi \nabla \times \boldsymbol{G}(\boldsymbol{r}, \boldsymbol{r'}) \boldsymbol{\alpha}_H \\ -i\xi \nabla \times \boldsymbol{G}(\boldsymbol{r}, \boldsymbol{r'}) \boldsymbol{\alpha}_E & \xi^2 \boldsymbol{G}(\boldsymbol{r}, \boldsymbol{r'}) \boldsymbol{\alpha}_H \end{pmatrix}, \tag{8}$$

where

$$\boldsymbol{G}(\boldsymbol{r}, \boldsymbol{r'}) = \left[\mathbf{1} + \frac{1}{\xi^2} \nabla \otimes \nabla \right] \frac{e^{i\xi |\boldsymbol{r} - \boldsymbol{r'}|}}{4\pi |\boldsymbol{r} - \boldsymbol{r'}|} \tag{9}$$

is the Dyadic Green's function and ξ is a dimensionless wave–number. To find the applied fields, $\phi(\boldsymbol{r}_n)$, we must impose the self–consistency condition

$$\boldsymbol{R}_{nm} \boldsymbol{\phi}_m = \boldsymbol{\phi}_{i,n}, \tag{10}$$

with $\boldsymbol{R}_{nm} = \mathbf{1}\delta_{nm} - G(\boldsymbol{r}_n, \boldsymbol{r}_m)$, $\boldsymbol{\phi}_m = \phi(\boldsymbol{r}_m)$ and $\boldsymbol{\phi}_{i,n} = \phi_i(\boldsymbol{r}_n)$. This forms a linear system that can be solved for the fields applied to the scatterers $\boldsymbol{\phi}_m$ using standard matrix methods. Once these are found, the fields (6) are fully specified.

To now design particular wave–shaping properties, we derive a way to iteratively move around the dipolar scatterers making up the metamaterial to optimise for a desired behaviour. Perturbatively expanding the position of each scatterer in the source terms of Maxwell's equations (4)

$$\begin{aligned} \delta(\boldsymbol{r} - \boldsymbol{r}_n - \delta\boldsymbol{r}_n) = \delta(\boldsymbol{r} - \boldsymbol{r}_n) \\ - (\delta\boldsymbol{r}_n \cdot \nabla)\delta(\boldsymbol{r} - \boldsymbol{r}_n) \\ + \frac{1}{2}(\delta\boldsymbol{r}_n \cdot \nabla)^2 \delta(\boldsymbol{r} - \boldsymbol{r}_n) + \ldots, \end{aligned} \tag{11}$$

we find an expression connecting a small change in the position of a scatterer to the small change induced in the fields

$$\delta\phi(\boldsymbol{r}) = G(\boldsymbol{r}, \boldsymbol{r}_n) \nabla\phi(\boldsymbol{r}_n) \cdot \delta\boldsymbol{r}_n. \tag{12}$$

From this we can analytically find gradients of figures of merit, which would be otherwise numerically expensive to evaluate. For example, consider a lensing problem where one wants the modulus squared of the field at a particular location $\boldsymbol{r}_\star$ to be maximised. The figure of merit is

$$\mathcal{F} = |\phi(\boldsymbol{r}_\star)|^2, \tag{13}$$

and the variation of the figure of merit to first under small changes in the fields is

$$\delta\mathcal{F} = 2\mathrm{Re}\left[\phi^*(\boldsymbol{r}_\star)\delta\phi(\boldsymbol{r}_\star)\right]. \tag{14}$$

Into this, we substitute the expression connecting the change in the field to a change in the position of a scatterer (12) to obtain an analytic expression for the gradient of the figure of merit with respect to all of the design variables i.e. the positions of the scatterers,

$$\frac{\partial\mathcal{F}}{\partial\boldsymbol{r}_n} = 2\mathrm{Re}\left[\phi^*(\boldsymbol{r}_\star) G(\boldsymbol{r}_\star, \boldsymbol{r}_n) \nabla\phi(\boldsymbol{r}_n)\right]. \tag{15}$$

While the gradient of the *fields* must still be calculated, the more expensive *figure of merit* gradient can be avoided. To evaluate the figure of merit gradient, one would have to manually vary the position of each scatterer in x and y one–by–one. In our framework the gradient can be evaluated for all scatterers in a single calculation, greatly improving the numerical efficiency. Once the gradients are found, gradient descent optimisation, with step size γ,

$$\boldsymbol{r}_n^{i+1} = \boldsymbol{r}_n^i + \gamma \frac{\partial\mathcal{F}}{\partial\boldsymbol{r}_n} \tag{16}$$

can be used to iteratively move the scatterers around to enhance a desired figure of merit.

Extending this to multi–functional systems requires us to form a composite figure of merit, which is a weighted sum of each of the figures of merit we would like to optimise

$$\mathcal{F} = \sum_i w_i F_i. \tag{17}$$

The overall gradient of this figure of merit can be calculated as before, so that

$$\frac{\partial\mathcal{F}}{\partial\boldsymbol{r}_n} = \sum_i w_i \frac{\partial F_i}{\partial\boldsymbol{r}_n}. \tag{18}$$

A sensible choice of the weights w_i is key to the success of the multi–objective optimisation. We motivate a choice of weights by considering the desired properties of the final device. We would like the optimisation to enhance each figure of merit equally: the designed device could not be described as multi–functional if one of the functions worked well and the other did not. Therefore, we choose the weights as

$$w_i \propto \frac{1}{F_i} \text{ , and normalised so that } \sum_i w_i = 1. \tag{19}$$

Over the course of the optimisation this means that an initially small figure of merit will have a larger weight and be prioritised so that by the end of the optimisation the performance of each figure of merit is equal.

In the following section we apply this framework to design i) a passive metamaterial structure that both enhances the efficiency of an emitter and shapes the radiation pattern in the desired way and ii) a structure that beams radiation in different directions depending on the polarisation of the emitter.

III. Example Devices

The first example we consider is the problem of distributing scatterers around an emitter to both increase the efficiency and re–shape the radiation pattern. Our figures of merit are therefore the power emission

$$F_1 = P = \frac{\omega}{2}\mathrm{Im}[\boldsymbol{p}^* \cdot \boldsymbol{E}(\boldsymbol{r'})]. \tag{20}$$

and overlap integral of the far–field Poynting vector $\boldsymbol{S}$ with the desired angular distribution $\psi_T(\theta)$

$$F_2 = I = \frac{\int d\theta |\boldsymbol{S}(\theta)| \psi_T(\theta)}{\sqrt{\int d\theta |\boldsymbol{S}(\theta)|^2} \sqrt{\int d\theta \psi_T^2(\theta)}}, \tag{21}$$

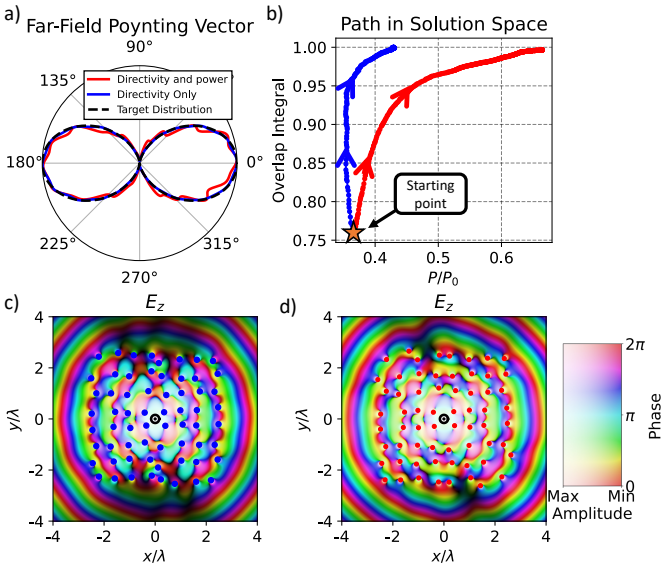

Fig. 1. Multi–objective optimisation solutions, seeking to increase the emitted power from a dipole while also shaping the far–field radiation pattern into the desired double–lobed shape. For comparison, the single–objective case, where only the radiation pattern is shaped is shown. a) shows the far–field radiation pattern in the plane of the multi–functional structure (red) as well as the target radiation pattern (black dashes). The case where only radiation pattern is shaped is shown in blue. In b), the paths in solution space of the single and multi–objective cases are shown. It is clear that our choice of weightings works well: both figures of merit undergo similar enhancements from their starting values. When only radiation pattern is controlled (blue line) power emission changes little over the optimisation, however when it is part of the composite figure of merit (red line) clear enhancement is seen at the same time as the overlap integral is increased. The single–objective structure is shown in c) and the multi–objective structure is shown in d), with the emitter polarised out of the page at the origin. In this example, we work at $\lambda = 550$ nm and the scatterers are silicon spheres of radius 65 nm.

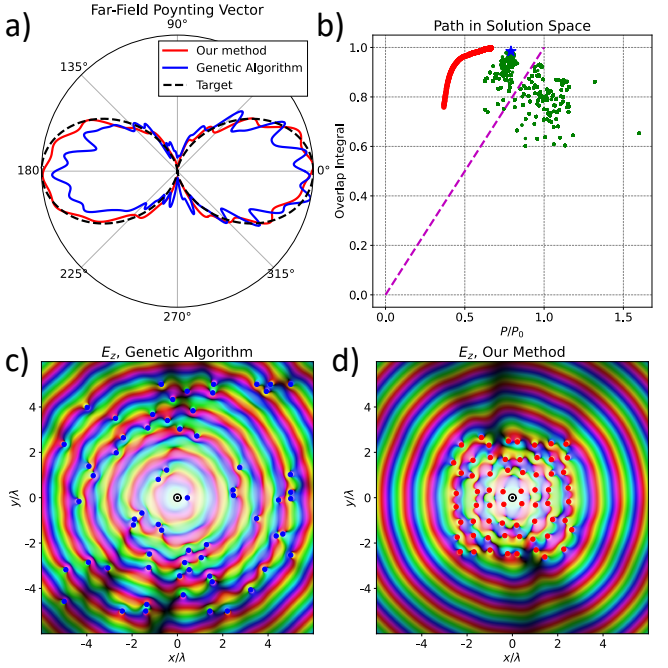

Fig. 2. A comparison of the results of our optimisation and a genetic algorithm seeking to shape a far–field radiation pattern while also improving efficiency. The far–field radiation patterns are compared in a), and the solution space paths are shown in b). The progress of our method is shown in red, and the progress of the genetic algorithm as green dots. Each dot represents a single population member. The final result of the genetic algorithm is shown as a blue star. The resulting structures are shown in c) and d).

where the angle θ is in the same plane as the metamaterial. In the example considered, we choose the target angular distribution to be

$$\psi_T(\theta) = \begin{cases} \cos^2\theta & 270° < \theta < 90°, \\ 0 & \text{otherwise.} \end{cases} \tag{22}$$

The result of the multi–objective optimisation using the framework presented in Section II is shown in Figure 1. In Figure 1 a) we plot the radiation pattern of the final device for both the single–objective problem, where only the radiation pattern was shaped and the multi–functional optimisation where power emission was also optimised. The matching of the far–field radiation pattern is slightly worse for the multi–objective case, due to the constraint that power also had to increase. From the path in solution space, Figure 1 b) it is evident that the multi–objective optimisation (shown in red) leads to a much larger enhancement in power than the single–objective case (blue). The designed structure for only shaping the far–field is given in Figure 1 c) and for the multi–objective case in Figure 1 d). The emitter is shown at the origin and is polarised out of the plane, so without the scattering structure the radiation pattern would be isotropic.

We compare the results of our multi–objective optimisation with a genetic algorithm. Genetic algorithms have been commonly used to design disordered structures of resonators to shape radiation from an emitter [8]. Using the differential evolution algorithm [9], with a population size of 20, and a maximum allowed iterations of 5000. The differential weight parameter is $F = 0.5$ and the crossover probability is CR = 0.7. This genetic algorithm was run several times and the best solution selected. The comparison between this result and the result of our optimisation is shown in Figure 2. Comparing the far–fields shown in Figure 2 a) we find that our method performs better than the genetic algorithm, although the genetic algorithm finds a result which increases power emission by more than our method, as can be seen in solution space Figure 2 b). The two designed structures are shown in Figure 2 c), d).

The second example we consider is that of a device that beams radiation into different directions depending upon the polarisation of the driven element. The operation of this device is shown in Figure 3. Our figures of merit are therefore

$$F_i = |\boldsymbol{S}(\theta_i)|. \tag{23}$$

We consider the source polarisation being either left or right circularly polarised, i.e.

$$\boldsymbol{p} = \frac{1}{\sqrt{2}} \begin{pmatrix} 1 \\ \pm i \\ 0 \end{pmatrix}. \tag{24}$$

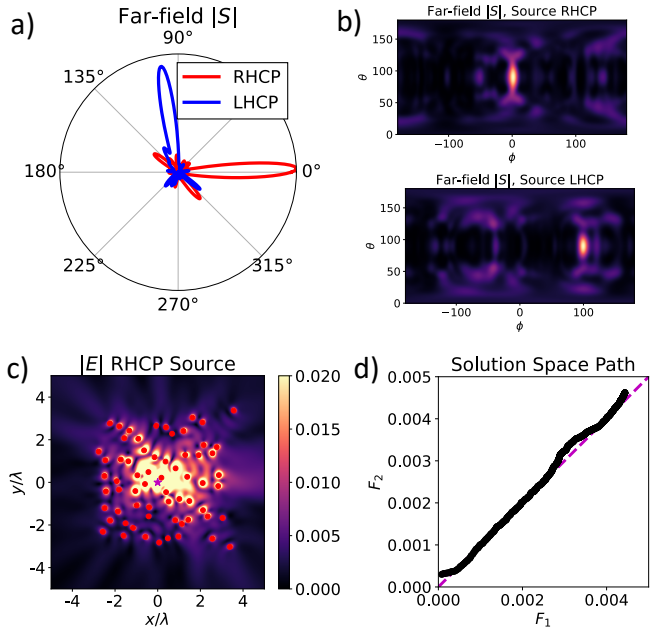

Fig. 3. Solution to the multi–objective problem of beaming in different directions based on the polarisation of the source. We work at optical wavelengths $\lambda = 550$ nm, using silicon spheres of radius 65 nm as the scatterers. a) shows the far–field Poynting vector in the plane of the metamaterial and b) shows the full far–field sphere. The aim was for a right handed source to beam into the 0° direction and for a left handed source to beam into the 100° direction. The optimised structure is shown in c) under a right–handed circular polarisation (RHCP) excitation. The emitter is indicated by a magenta star at the origin. The path in solution space of the optimisation, d), shows that over the optimisation both figures of merit are enhanced equally, due to our choice of weights.

The Poynting vector can then be expanded to first order to find the derivatives of the figures of merit for the optimisation procedure. Figure 3 a) shows the radiation patterns of the designed structure excited by each of the two different sources we consider. For a right-handed source, the target angle is $\theta = 0°$ and for a left–handed source, $\theta = 100°$. The far–field Poynting vector in the plane of the metamaterial, Figure 3 a), also shows clear peaks at the desired locations, which are also evident in the near–fields shown in Figure 3 c). The path in solution space, Figure 3 d), shows that the choice of weighting has ensured that the performance of both figures of merit remain similar over the optimisation and in the final result.

IV. Conclusion

Building upon recent developments in designing metamaterials using the discrete dipole approximation, we have developed a versatile semi–analytic framework for designing multi–functional metamaterials to shape antenna radiation. We have applied this framework to design two devices: one which re–shapes the radiation pattern of an emitter while also enhancing the efficiency, and one which beams radiation into different directions depending upon the polarisation of a driven element. The devices we propose are straightforward to fabricate as dielectric does not need to be graded in space, instead one must only distribute identical scatterers around an emitter.

Our approach could be utilised to design very wide classes of multi–functional devices. While we have worked at optical wavelengths, with a different choice of resonators this framework could be applied to design microwave or mm–wave devices. In addition, this methodology could be applied to engineer other figures of merit such as radar cross–sections.

Acknowledgment

We acknowledge financial support from the Engineering and Physical Sciences Research Council (EPSRC) of the United Kingdom, via the EPSRC Centre for Doctoral Training in Metamaterials (Grant No. EP/L015331/1). J.R.C also wishes to acknowledge financial support from Defence Science Technology Laboratory (DSTL). S.A.R.H acknowledges financial support from the Royal Society (URF\R\211033)

References

[1] S. Molesky, Z. Lin, A. Y. Piggott, W. Jin, J. Vucković and A. W. Rodriguez, “Inverse design in nanophotonics” Nature Photon. , vol. 12, pp. 659–670, 2018.

[2] A. Y. Piggott, J. Lu, K. G. Lagoudakis, J. Petykiewicz, T. M. Babinec and J. Vučković, “Inverse design and demonstration of a compact and broadband on-chip wavelength demultiplexer” Nature Photon. , vol. 9, pp. 374–377, 2015.

[3] S.-Q. Li and X. Xu and R. M. Veetil and V. Valuckas and R. Paniagua-Domínguez and A. I. Kuznetsov, “Phase-only transmissive spatial light modulator based on tunable dielectric metasurface” Science , vol. 364, pp. 1087-1090, 2019.

[4] D. Pande, J. Gollub, R. Zecca, D. L. Marks and D. R. Smith, “Symphotic Multiplexing Medium at Microwave Frequencies” Phys. Rev. Applied , vol. 13, 024033, 2020.

[5] C. M. Lalau-Keraly and S. Bhargava and O. D. Miller and E. Yablonovitch, “Adjoint shape optimization applied to electromagnetic design” Opt. Express , vol. 21, pp. 21693-21701, 2013.

[6] J. R. Capers, S. J. Boyes, A. P. Hibbins and S. A. R. Horsley, “Designing the collective non-local responses of metasurfaces” Commun. Phys., vol. 4, 209, 2021.

[7] J. R. Capers, S. J. Boyes, A. P. Hibbins and S. A. R. Horsley, “Designing Metasurfaces to Manipulate Antenna Radiation” Proc. SPIE 12130, Metamaterials XIII, 121300H, 2022.

[8] P. R. Wiecha, A. Arbouet, A. Cuche, V. Paillard and C. Girard, “Decay rate of magnetic dipoles near nonmagnetic nanostructures” Phys. Rev. B, vol 97, 085411, 2019.

[9] R. Storn and K. Price, “Differential Evolution – A Simple and Efficient Heuristic for global Optimization over Continuous Spaces” J Glob. Optim., vol 11, pp. 314-359, 1997.